View metadata, citation and similar papers at core.ac.uk

brought to you by CORE

provided by E-resource repository of the University of Latvia

IOP Conference Series: Materials Science and Engineering

**PAPER** • **OPEN ACCESS**

# Luminescence characteristics of magnesium aluminate spinel crystals of different stoichiometry

To cite this article: G Prieditis *et al* 2019 *IOP Conf. Ser.: Mater. Sci. Eng.* **503** 012021

View the article online for updates and enhancements.

This content was downloaded from IP address 77.219.11.214 on 08/07/2020 at 11:41

# Luminescence characteristics of magnesium aluminate spinel crystals of different stoichiometry

**G Prieditis[1,a], E Feldbach[1], I Kudryavtseva[1], A I Popov[2b], E Shablonin[1] and A Lushchik[1,c]**

[1]Institute of Physics, University of Tartu, W. Ostwald 1, 50411 Tartu, Estonia
[2]Institute of Solid State Physics, University of Latvia, Kengaraga 8, Riga LV-1063, Latvia

E-mail: [a]prieditisgatis@gmail.com, [b]popov@latnet.lv, [c]aleksandr.lushchik@ut.ee

**Abstract.** Magnesium aluminate spinel single crystals with different stoichiometry, $MgAl_2O_4$ (1:1 spinel) and $MgO{\cdot}2.5Al_2O_3$ (1:2.5) were investigated using different optical methods (cathode-, photo- and thermally stimulated luminescence (TSL), optical absorption, "creation spectra" of TSL peaks and phosphorescence by VUV radiation). Low-temperature charge carrier traps and the position of intrinsic UV emission bands depend on the degree of stoichiometry. Antisite defects (ADs), $Mg^{2+}$ or $Al^{3+}$ located in a "wrong" cation site ($Mg|_{Al}$ or $Al|_{Mg}$) are the main as-grown structural defects, which serve also as efficient traps for electrons and holes as well as seeds for bound excitons. AD concentration is especially high in 1:2.5 spinel. There are several manifestations of ADs (electronic excitations near ADs) in the spectral region of 7–7.5 eV, slightly below the energy gap.

## 1. Introduction

Magnesium aluminate spinel is a fascinating material applicable for various applications in science and technology [1]. Its particular feature is a very high tolerance against radiation and absence of swelling even after heavy fast-neutron irradiation (see, e.g., [2,3]). Therefore, $MgAl_2O_4$ crystals and transparent ceramics are considered as attractive candidates for diagnostics/optical windows in future fusion projects (ITER, DEMO, PROTO, industrial reactors) [4]. It is generally accepted that the functionality of optical components strongly depends on the concentration of as-grown structural defects and their accumulation during material exposure to dense and prolonged irradiation.

Mg-Al spinel is a mixed double oxide $MgO{\cdot}nAl_2O_3$ and may be regarded as a face-centered cubic structure formed by closely packed oxygen ions. In equimolar mixture of binary oxides – stoichiometric $MgAl_2O_4$ (melting temperature 2400 K), $Mg^{2+}$ ions occupy every eighth tetrahedral (*T*) interstice and a half of octahedral (*O*) ones are filled by $Al^{3+}$ in each unit cell. In a "normal" $MgAl_2O_4$, there is no cation disorder, while the exchanging of cations between *T* and *O* sites results in the formation of so-called antisite defects (ADs) – $Mg|_{Al}$ or $Al|_{Mg}$ – a cation in a "wrong" position. The formation energy of these ADs in $MgAl_2O_4$ is much lower than the one for all other point defects [5].

The presence of ADs charged -1 or +1 with respect to a regular lattice determines the degree of cation disorder ascribed by inversion parameter *i*. In a fully inversed spinel ($i = 1$), all $Mg^{2+}$ are located in $Al^{3+}$ sites, i.e. are ADs. In nonstoichiometric spinel, for instance $MgO{\cdot}2.5Al_2O_3$ Al-rich crystals studied in the present work, some $Al^{3+}$ replace $Mg^{2+}$ with the creation of positively charged $Al|_{Mg}$, while additional

Content from this work may be used under the terms of the Creative Commons Attribution 3.0 licence. Any further distribution of this work must maintain attribution to the author(s) and the title of the work, journal citation and DOI.
Published under licence by IOP Publishing Ltd

cation vacancies (mainly *O*-coordinated, i.e. aluminium vacancies $V_{Al}$) are formed for charge compensation [6].

There are many experimental and modelling studies related to the structural damage of radiation-tolerant Mg-Al spinel crystals exposed to dense irradiation of different types – high-energy electrons, fast neutrons, swift heavy ions (see [3,5,7-12] and references therein). On the other hand, the concentration of as-grown structural defects (mainly ADs or AD-containing complex defects) in the majority of Mg-Al single crystals is rather high; $i$ reaches 0.1–0.2 in our 1:1 samples (determined by XRD in accordance with [13]) and is even higher in transparent optical ceramics. Therefore, the present study is devoted to the optical characterization of as-grown structural defects in stoichiometric and nonstoichiometric Mg-Al spinel crystals.

## 2. Experimental details

Single crystals of stoichiometric $MgAl_2O_4$ (labelled as 1:1 spinel) were grown by Union Carbide Corporation using the Czochralski method and nonstoichiometric $MgO{\cdot}2.5Al_2O_3$ samples (1:2.5 spinel) were grown using the Verneuil method. Both samples contained Cr, Mn and Fe impurities.

Cathodoluminescence (CL) measurements (see for details [14,15]) were performed using an electron gun operating at 10 keV and 2.5 μA and a close-cycle He cryostat. CL was analyzed using vacuum double monochromator built up at the Institute of Physics, Tartu. After the electron irradiation was stopped, it was possible to register the spectra of phosphorescence at 6 K and the thermally stimulated luminescence (TSL) at 6–420 K (heating rate of $\beta = 10$ K min$^{-1}$) for an integral signal or a specific monochromator-selected emission.

The spectra of optical absorption in UV-VUV spectral region were measured at room temperature (RT) using a homemade setup based on a single vacuum monochromator VMR-2. The number of incident photons from the hydrogen discharge in a flow capillary tube was maintained constant by varying the monochromator slit width and using the constant signal from sodium salicylate for normalization. The "creation spectra" of several TSL peaks ($\beta = 10$ K min$^{-1}$, 80–450 K) and phosphorescence by selective VUV radiation (prescribed number of exciting photons at each of several energies) were measured using the same setup and highly sensitive methods elaborated in Tartu earlier (see, e.g., [16,17]).

For photoluminescence (PL) measurements, a Hamamatsu deuterium discharge lamp was used as excitation source, McPherson vacuum and ANDOR Shamrock monochromators, a photon counting head and close-cycle He cryostat. The excitation spectra were normalized to equal the quantum intensities of the radiation falling onto the crystal (a sodium salicylate was used as a reference signal).

## 3. Results and Discussion

Figure 1*a* presents the spectra of CL measured for 1:1 and 1:2.5 spinel single crystals at various temperatures. The general spectrum shape is similar, but the spectra still differ, to some extent, in stoichiometric and nonstoichiometric crystals. At 6–78 K, the CL is more intense (by more than five times for UV luminescence band) in the 1:1 spinel, and the attenuation of CL, especially in UV spectral region, takes place with the temperature rise to RT.

Based on the literature data ([12,18–23] and references therein), the emission bands peaked at ~1.8 and ~2.4 eV can be ascribed to $Cr^{3+}$ and $Mn^{2+}$ impurity ions, respectively, while some of UV bands are of intrinsic origin partly related to ADs (excitonic type and recombination luminescence). Based on the similarity to MgO and $Al_2O_3$ crystals being constituent parts of spinel, the emission bands around 3 eV can be partly related to F and $F^+$ centers (two or one electron in the field of an oxygen vacancy $V_O$). These F- and $F^+$-emissions should be well pronounced in the crystals exposed to dense irradiation providing knock-on (impact) creation of novel F and $F^+$. Nevertheless, in as-grown (virgin) spinel crystals, there can exist a certain amount of $V_O$, and the emission of $F^+$ and/or F centers appears due to

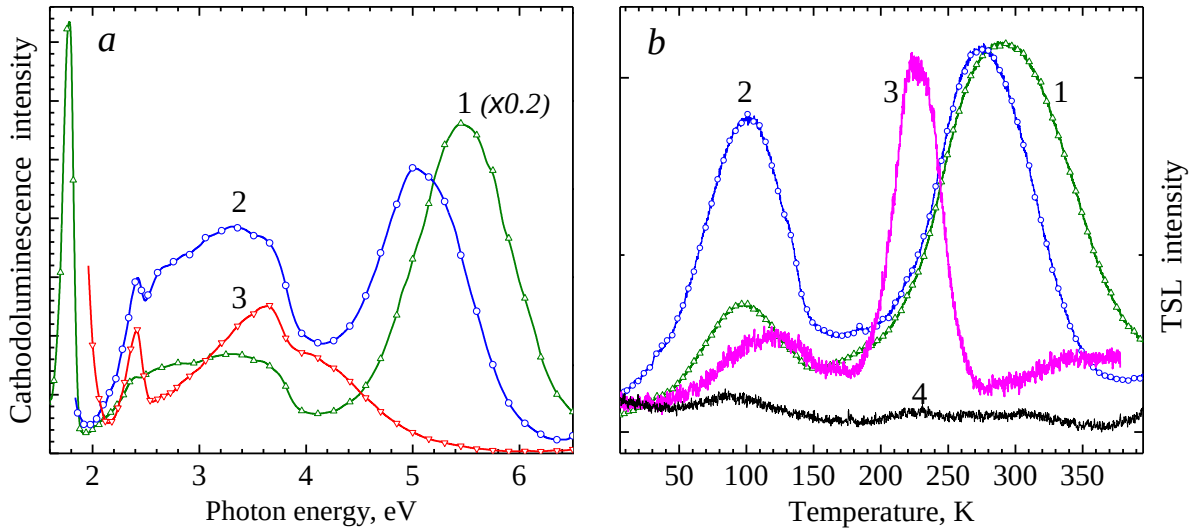


**Figure 1.** *a* – Cathodoluminescence spectra measured for virgin $MgAl_2O_4$ (curve 1) and $MgO{\cdot}2.5Al_2O_3$ (2 and 3) single crystals under excitation by 10 keV electrons at 78 K (1), 6 K (2) and RT (3). *b* – TSL curves measured after irradiation of virgin 1:1 (curves 1 and 2); virgin 1:2.5 (curve 3) and neutron-irradiated 1:2.5 (curve 4) samples by an10-keV electron beam at 6 K. $\beta = 10$ K min$^{-1}$.

the interaction of electrons and holes (*e-h* pairs), formed under electron beam excitation, with $V_O$ (for details see, e.g., [15, 24]). To the best of our knowledge, up to now only the ~2.7-eV emission is reliably interpreted as the $F^+$-center emission [21], which is relatively intense in our 1:2.5 spinel crystal.

The presence of as-grown structural defects can be also visualized measuring TSL of the crystals exposed to 10-keV electron irradiation, i.e. after prolonged CL measurements. Electrons of such energy are not able to form novel structural defects, while already existing as-grown structural defects (as well as some impurities) serve as efficient electron/hole traps for *e-h* formed by an electron beam. Figure 1*b* shows the normalized TSL curves measured at a heating of the 1:1 and 1:2.5 spinel single crystals previously irradiated by 10-keV electrons at 6 K. It is clearly seen that different TSL peaks dominate in two 1:1 samples from different suppliers and the 1:2.5 crystal. This circumstance testifies to the different type/concentration of as-grown structural defects (incl. charged ADs - $Mg|_{Al}$ and $Al|_{Mg}$) in the crystals with different stoichiometry. The analysis of the detected TSL peaks is still in the progress. The first order kinetics gives rather "strange" results due to complex and unusual origin of the TSL peaks in spinel crystals with high level of structural disorder (see also text related to Figure 3). Note that TSL in a fast-neutron irradiated 1:2.5 crystal measured under the same conditions is strongly suppressed. The same situation occurs if we compare CL spectra for the virgin and neutron irradiated crystals (see also [12,15]). Such luminescence attenuation is mainly caused by CL reabsorption by neutron-induced defects (e.g., F and $F^+$ centers) but the contribution of radiation-induced enhancement of lattice inversion cannot be excluded as well.

A set of emission spectra was measured at the photoexcitation (from 6 to 8.1 eV) of different spinel samples at RT or 6 K. As an example, Figure 2*a* presents some PL spectra for two 1:1 spinel samples at 6 K. There is a certain similarity with the CL spectra presented in Figure 1*a*. At RT, the intense phosphorescence (PhP), detectable after the excitation had been stopped, was registered in the sample preliminary excited with photons of $h\nu >$ ~7.5 eV (see text related to Figure 3*b*). The PhP spectrum for the 1:1 crystal excited by 8.1-eV photons is presented in Figure 2*a* (curve 3). Such intense PhP disturbs the spectra of PL excited by photons from the region of fundamental absorption and artificially increases the PL intensity in UV region (see curve 1′*a*). At helium temperatures, PhP is generally weak and practically absent in UV region, while the intensity of UV photoluminescence increases similar to the case of CL. It is also worth noting that the role of PhP is underestimated yet.

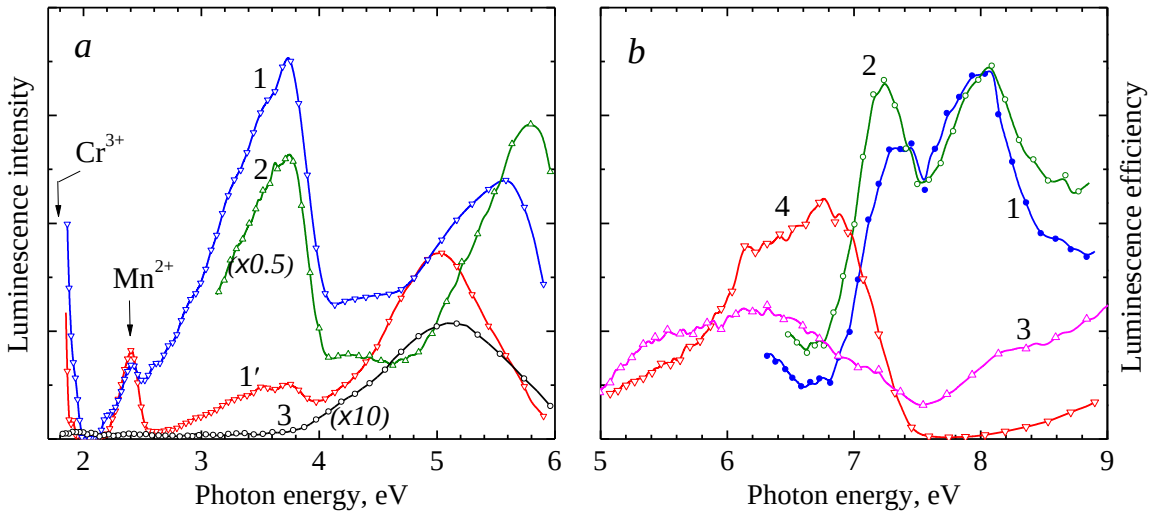


**Figure 2.** *a* – Emission spectra measured for two different 1:1 single crystals at the excitation by 8.1-eV photons at 6 K (curves 1 and 2) and RT (1'). Spectrum of phosphorescence measured at RT for the 1:1 crystal previously excited by 8.1-eV photons (curve 3, multiplied by a factor of 10). *b* – Excitation spectra for the emission measured at 5.3 eV (curve 1), 4.6 eV (2), 2.3 eV (3) and 1.8 eV (4) at 6 K.

Figure 2*b* presents the excitation spectra of different emissions measured for the 1:1 spinel crystal at 6 K. Based on these excitation spectra, two groups of emissions can be clearly separated. Firstly, impurity emissions of $Mn^{2+}$ and $Cr^{3+}$ (similar to CL spectra, peaks at 2.4 and ~1.8 eV, respectively) are efficiently excited strongly below the region of fundamental absorption (energy gap in $MgAl_2O_4$ at 6 K is expected around 8.1 eV). After emission spectra corrections, $Cr^{3+}$ emission is too strong, dominates over other ones and is not shown in Figure 2*a*. Secondly, UV emissions above 3.5 eV have main excitation bands at ~7.2 eV and ~8 eV (excitation spectra for 4.6- and 5.3-eV emission are shown in figure) and can be considered as the intrinsic emissions of Mg-Al spinel crystals (see, e.g., [22]). The behavior of the 3.7-eV emission (not shown in Figure 2*b*) is more complicated, it is excited by photons of $h\nu < 7$ eV as well, but, in our opinion, can be related to ADs. Because of the overlapping of wide emission bands, the precise analysis of the origin of tentatively intrinsic emissions is rather complicated and should be continued. Nevertheless, the analysis of experimental PL data and similarity with $Y_3Al_5O_{12}$ and $Lu_3Al_5O_{12}$ single crystals ([25-28] and references therein) allow to suggest that the ~7.2 eV excitation band in our virgin spinel samples can be tentatively ascribed to ADs.

Figure 3*a* shows the fragments of TSL curves measured after irradiation of the 1:1 single crystal by 8-eV photons at 80 K or 270 K. Such photoexcitation leads to the appearance of the TSL peak at ~130 K and some other peaks at higher temperatures. Note that the low-temperature peak is located at higher temperature than that detected after electron irradiation at 6 K. Probably, higher temperature of photoexcitation as well as its low intensity causes such shift of the peak position. Similar to the case of crystal irradiation with an electron beam, the low-temperature TSL peak has a complex origin and cannot be approximated by the first order kinetics (extremely low values of frequency factor).

Figure 3*b* demonstrates the creation spectrum of the ~130 K TSL peak measured for the 1:1 crystal irradiated by a prescribed number of the exciting photons at each of several energies of 6.4–8.0 eV at 80 K. After every isodose irradiation, TSL was measured up to 450 K and the light sum of the 130 K peak (or peak intensity) was used for the construction of the "creation spectrum" reflecting the efficiency of the TSL peak induced by photons of different energies. The efficiency of TSL is high after the 1:1 crystal irradiation by photons of ~7–8 eV. Charge carriers needed for the further appearance of TSL could arise due to the formation of bound excitons localized, respectively, near negatively and positively charged $Mg|_{Al}$ and $Al|_{Mg}$ ADs as well as due to the beginning of band-to band transitions.

According to Figure 3*b*, this creation spectrum of the 130-K TSL peak is similar to the excitation (creation) spectrum of PhP for the same 1:1 sample (curve 2). In the latter case, the decay of PhP was

recorded after an isodose irradiation by photons with a certain energy had been stopped. The PhP is detectable if the sample was previously excited by photons with the energy from 7 eV up to the edge of fundamental absorption around 8 eV (see transmission spectrum – curve 3). The measure of PhP was estimated via light sum of a signal, spectrally integrated or selected by an optical filter (3.2–5.1 eV) as well as the intensity measured after a certain time delay after the photoexcitation had been stopped. The shapes of PhP excitation/creation spectra coincide well for all three used registration methods.

Both creation spectra allow to elucidate the energy region of the exciting photons which cause a sequent appearance of conduction electrons/holes – either released from traps/structural defects or formed due to band-to band-transitions. It was mentioned already that ADs in $MgAl_2O_4$ are charged defects and serve as the traps for charge carriers. In particular, electrons can be released from $Al|_{Mg}$ with the corresponding optical absorption slightly above 7 eV (see also [12]). The similar situation has been earlier detected for ADs in $Lu_3Al_5O_{12}$ [26]. The sharp rise of PhP efficiency at $h\nu >$ 7.5 eV can testify to the beginning of band-to-band transitions in the 1:1 spinel crystal at 270 K, while the efficiency decrease at $h\nu >$ 7.7–7.8 eV reflects negligible penetration depth of such exciting photons (see transmittance spectrum in Figure 3*b*).

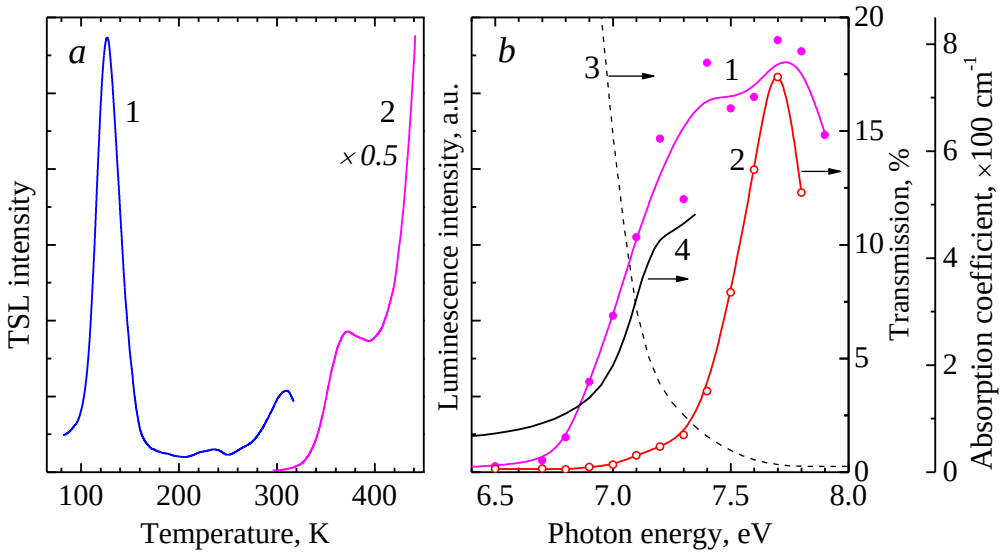


**Figure 3.** ***a*** – TSL curves measured for the 1:1 crystal irradiated by 8-eV photons at 80 K (curve 1) or 270 K (curve 2). ***b*** – Creation spectrum of the 130-K TSL peak by VUV radiation at 80 K (curve 1), excitation spectrum for phosphorescence (integral signal, curve 2) and transmission spectrum (3) for the 1:1 crystal at 270 K. Absorption spectrum of the 1:2.5 crystal (thickness of 0.1 mm) at RT (4).

Figure 3*b* also demonstrates the absorption spectrum measured in UV-VUV spectral region for an as-grown 1:2.5 crystal. Absorption coefficient in this spectral region has very high values, therefore the sample with thickness of 0.1 mm was used for this measurement. There is a clearly observed shoulder at 7.2 eV (less pronounced but still detectable in the 1:1 spinel), which was also detected in the excitation spectra of PL and tentatively ascribed to ADs (bound excitons near ADs, Figure 2*b*). Our previously obtained data on radiation-induced optical absorption in $MgAl_2O_4$ confirm the relation of the shoulder at ~7.2 eV to ADs being a constituent part of a number of the revealed paramagnetic defects, thermal annealing of which correlates with the attenuation of the 7.2-eV band of radiation-induced absorption [12]. As it was mentioned already, the concentration of ADs in the 1:2.5 nonstoichiometric crystal is significantly higher than that in the 1:1 crystal.

## 4. Conclusions

Manifestations of as-grown structural defects have been revealed in magnesium aluminate spinel single crystals with different stoichiometry by means of different optical methods. The main defects in virgin 1:1 and 1:2.5 spinel crystals are antisite defects – $Mg^{2+}$ or $Al^{3+}$ located in a “wrong” cation site,

$Mg|_{Al}$ or $Al|_{Mg}$. These ADs are charged with respect to the perfect lattice and serve as electron/hole traps or "stickers" for exciton-like electron excitations (bound excitons). Carrier traps manifest themselves via TSL arising at heating of the crystals irradiated with an electron beam or photons. Based on the excitation spectra of different emissions, optical absorption spectra as well as the "creation spectra" of TSL peaks by VUV radiation, the spectral region at ~7–7.5 eV, slightly below the energy gap, can be tentatively ascribed to ADs, the number of which is especially high in the 1:2.5 spinel single crystals. This suggestion is also confirmed by our previous study on radiation-induced defects (including ADs) in fast-neutron irradiated Mg-Al spinel crystals [12]. The excitation/creation spectrum of phosphorescence indicates on the beginning of interband transitions above 7.5 eV in $MgAl_2O_4$ at 270 K.

## 5. Acknowledgments

We are grateful to Drs E. Vasil'chenko and A. Maaroos for the help with experiments and useful discussions. This work has been carried out within the framework of the EUROfusion Consortium and has received funding from the Euratom research and training programme 2014-2018 under grant agreement No 633053. The views and opinions expressed herein do not necessarily reflect those of the European Commission. In addition, the research leading to these results has received funding from the Estonian Research Council – Institutional Research Funding IUT02-26.

## 6. References

[1] Ganesh I 2013 *Int. Mater. Rev*. **58** 63
[2] Clinard Jr F W, Hurley G F and Hobbs L W 1982 J. *Nucl. Mat.* **108-109** 655
[3] Sickafus K E, Minervini L, Grimes R W, Valdez JA, Ishimaru M, Li F, McClellan K J and T. Hartmann 2000 *Science* **289** 748
[4] Gonzales de Vicente S M, Hodgson E R and Shikama T 2017 *Nucl. Fusion* **57** 092009
[5] Gilbert A, Smith R, Kenny S D, Murphy S T, Grimes R W and Ball J A 2009 *J. Phys.: Condens. Matter* **21** 275406
[6] Dupree R, Lewis M H and Smith M E. 1986 *Phil. Mag. A* **53** L17
[7] Summers G P, White G S, Lee K H and Crawford J H 1980 *Phys. Rev. B* **21** 2578
[8] Bacorisen D, Smith R, Uberuaga B P and Sickafus K E 2006 *Phys. Rev. B* **74** 214105
[9] Zinkle S J 2012 *Nucl. Instrum. Meth. B* **286** 4
[10] Costantini J-M, Leiong G, Guillaumet M, Weber W J, Takaki S and Yasuda K 2016 *J. Phys.: Condens. Matter* **28** 325901
[11] Mironova-Ulmane N, Skvortsova V, Pavlenko A Feldbach E, Lushchik A, Lushchik Ch, Churmanov V, Ivanov D, Ivanov V and Aleksanyan E 2016 *Radiat. Meas*. **90** 122
[12] Lushchik A, Dolgov S, Feldbach E Pareja R, Popov A I, Shablonin E and Seeman V 2018 *Nucl. Instrum. Meth. B* **435** 31
[13] Ball J A, Pirzada M, Grimes R W, Zacate M O, Price D W and Uberuaga B P 2005 *J. Phys.: Condens. Matter* **17** 7621
[14] Nakonechnyi S, Karner T, Lushchik A, Lushchik Ch, Babin V, Feldbach E, Kudryavtseva I, Liblik P, Pung L and Vasil'chenko E 2006 *J. Phys: Condens. Mat.* **18** 379
[15] Feldbach E. Tõldsepp E, Kirm M, Lushchik A, Mizohata K and Räisänen J 2016 *Opt. Mater*. **55** 164
[16] Lushchik A, Feldbach E, Frorip A, Ibragimov K, Kuusmann I and Lushchik C 1994 J. *Phys.: Condens. Mat.* **6** 2357
[17] Lushchik A, Kudryavtseva I, Lushchik Ch, Vasil'chenko E, Kirm M and Martinson I 1995 *Phys. Rev. B* **52** 10069
[18] Skvortsova V, Mironova-Ulmane N and Ulmanis U 2002 *Nucl. Instrum. Meth. B* **191** 256
[19] Gritsyna V T, Afanasyev-Charkin I V, Kazarinov Yu G and Sickafus K E 2004 *Nucl. Instrum. Meth. B* **218** 264
[20] Gritsyna V T, Kazarinov Yu G, Kobyakov V A and Reimanis I E 2006 *Nucl. Instrum. Meth. B* **250** 342
[21] Sawai S and Uchino T 2012 *J. Appl. Phys*. **112** 103523

[22] Jozwik I, Jagielski J, Gawlik G, Jozwik P, Ratajczak R, Panczer G, Moncoffre N, Wajler A, Sidorowicz A and Thomé L 2016 *Phys. Chem. Minerals* **43** 439
[23] Lushchik A, Kirm M, Kotlov A, Liblik P, Lushchik Ch, Maaroos A, Nagirnyi V, Savikhina T and Zimmerer G 2003 J. Lumin. **102-103** 38
[24] Lushchik A, Lushchik Ch, Schwartz K, Vasil'chenko E, Kärner T, Kudryavtseva I, Isakhanyan V and Shugai A 2008 *Nucl. Instrum. Meth. B* **266** 2868
[25] Nikl M, Laguta V V and Vedda A 2008 *Phys. Status Solidi B* **245** 1701
[26] Babin V, Laguta V V, Makhov A, Nejezchleb K, Nikl M and Zazubovich S 2008 *IEEE Trans. Nucl. Sci.* **55** 1156
[27] Lushchik A, Kärner T, Lushchik Ch, Schwartz K, Savikhin F, Shablonin E, Shugai A and Vasil'chenko E 2012 *Nucl. Instrum. Meth. B* **286** 200
[28] Lushchik A, Lushchik Ch, Popov A I, Schwartz K, Shablonin E and Vasil'chenko E 2016 *Nucl. Instrum. Meth. B* **374** 90

Institute of Solid State Physics, University of Latvia as the Center of Excellence has received funding from the European Union's Horizon 2020 Framework Programme H2020-WIDESPREAD-01-2016-2017-TeamingPhase2 under grant agreement No. 739508, project CAMART²